Published in final edited form as:
Cell Stem Cell. 2010 May 7; 6(5): 421–432. doi:10.1016/j.stem.2010.02.018.

Integrin alpha 6 regulates glioblastoma stem cells

Justin D. Lathia[1], **Joseph Gallagher**[1], **John M. Heddleston**[1], **Jialiang Wang**[2], **Christine E. Eyler**[1,3], **Jennifer MacSwords**[1], **Qiulian Wu**[1], **Amit Vasanji**[4], **Roger E. McLendon**[5], **Anita B. Hjelmeland**[1], and **Jeremy N. Rich**[1]

[1]Department of Stem Cell Biology and Regenerative Medicine, Cleveland Clinic, Cleveland, Ohio 44195, USA.

[2]Department of Surgery, Duke University Medical Center, Durham, North Carolina 27705, USA.

[3]Department of Pharmacology and Cancer Biology, Duke University Medical Center, Durham, North Carolina 27705, USA.

[4]Image Processing Core, Cleveland Clinic, Cleveland, Ohio 44195, USA.

[5]Department of Pathology; Duke University Medical Center, Durham, North Carolina 27705, USA.

Summary

Cancer stem cells (CSCs) are a subpopulation of tumor cells suggested to be critical for tumor maintenance, metastasis, and therapeutic resistance. Prospective identification and targeting of CSCs are therefore priorities for the development of novel therapeutic paradigms. While CSC enrichment has been achieved with cell surface proteins including CD133 (Prominin-1), the roles of current CSC markers in tumor maintenance remain unclear. We examined the glioblastoma stem cell (GSC) perivascular microenvironment in patient specimens to identify enrichment markers with a functional significance and identified integrin α6 as a candidate. Integrin α6 is co-expressed with conventional GSC markers and enriches for GSCs. Targeting integrin α6 in GSCs inhibits self-renewal, proliferation, and tumor formation capacity. Our results provide evidence that GSCs express high levels of integrin α6, which can not only serve as an enrichment marker but also as a promising anti-glioblastoma therapy.

Introduction

Cancers are complex biological systems which contain neoplastic and non-neoplastic cells along with vasculature, inflammatory cells, and associated stroma (Hanahan and Weinberg, 2000). In the neoplastic compartment, some tumors contain cellular fractions capable of initiating tumors similar to the parental tumor when transplanted into a secondary site. This fraction of cells, referred to as cancer stem cells (CSCs), tumor initiating cells, or tumor propagating cells has been found in many tumors (Reya et al., 2001), including brain cancers (Bao et al., 2006a; Bao et al., 2006b; Galli et al., 2004; Hemmati et al., 2003; Ignatova et al., 2002; Singh et al., 2003; Singh et al., 2004; Taylor et al., 2005; Yuan et al., 2004). Gliobastoma mutliforme (GBM) is the most common and lethal primary brain tumor with

Correspondence: Jeremy N. Rich, MD Department of Stem Cell Biology and Regenerative Medicine Cleveland Clinic 9500 Euclid Avenue, Mailstop NE30 Cleveland, OH 44195 USA Phone: +1 216 636 0790 Fax: +1 216 636 5454 richj@ccf.org.

less than 3% 5-year survival rate (Stupp et al, 2005). Recent experimental evidence from our laboratory and others has suggested the CSC population can be a potential therapeutic target. Glioblastoma stem cells (GSCs) are relatively radioresistant (Bao et al., 2006a) and chemoresistant (Liu et al., 2006). GSCs activate a number of key stem cell signaling pathways, including Akt, bone morphogenetic protein, c-myc, hypoxia response, Notch, Sonic Hedgehog (Bar et al., 2007; Eyler et al., 2008; Fan et al., 2006; Li et al., 2009; Piccirillo et al., 2006; Wang et al., 2008b).

Critical to GSC research is their prospective identification and isolation from tumor tissue. Many studies have relied on the enrichment of GSCs based on expression of the cell surface protein CD133 (prominin-1) (see review by Bidlingmaier et al., 2008), which has also been used as a selection marker for neural stem cells (Uchida et al., 2000). However, CD133 faces limitations as recent reports have shown that CD133 negative GBM cells can form tumors (Beier et al., 2007; Joo et al., 2008; Wang et al., 2008a) and the expression of CD133 may be cell cycle regulated (Jaksch et al., 2008). These issues underscore the need for additional markers to identify GSCs of which several have been proposed (L1CAM, A2B5, CD15 (Bao et al., 2008; Ogden et al., 2008; Read et al., 2009; Son et al., 2009)). An alternative strategy for the identification of GSC markers and possible therapeutic targets could be based on examination of the perivascular microenvironment in which GSCs reside (Calabrese et al., 2007). Extracellular matrix (ECM) proteins are key structural components of the perivascular niche and regulate normal stem cell and tumor proliferation and migration (Gilbertson and Rich, 2007). The ECM modulates cell behavior via the heterodimer integrin cell surface receptors, which consist of α and β subunits (Hynes, 2002). Integrins direct development as demonstrated by the severe phenotypes displayed by many integrin knockout models (Schmid and Anton, 2003), including brain phenotypes (Georges-Labouesse et al., 1998; Graus-Porta et al., 2001). Recently, selection based on integrins has been used to enrich for normal neural stem/progenitor cells (Lathia et al., 2007b; Hall et al., 2006), as well as CSCs from the breast (Vaillant et al., 2008) and prostate (Patrawala et al., 2007).

Of particular interest to stem cell biology has been integrin α6, the receptor for the ECM protein laminin, which forms heterodimers with integrin β1 or β4. Integrin α6 is highly expressed in embryonic, hematopoeitic, and neural stem cells (Fortunel et al., 2003). In the brain, laminins and integrin α6β1 regulate neural stem cell growth (Hall et al., 2008) and play a pivotal role in maintaining adhesion to the ventricular zone, ensuring proper neural stem cell division (Loulier et al., 2009). Laminin is also a key component in culturing relatively pure adherent GSC cultures, suggesting a critical role for the laminin-integrin relationship in GSC maintenance (Fael Al-Mayhani et al., 2009; Pollard et al., 2009). With the importance of integrin α6 in neural stem cells, the perivascular localization of GSCs enriched in ECM, and use of laminin to propagate GSC cultures, we hypothesized that integrin α6 may serve as a functional marker of GSCs.

Results

Integrin α6 marks the glioblastoma perivascular niche

While previous studies have evaluated integrin α6 in normal astrocytes (Aloisi et al., 1992; Paulus et al., 1993) and gliomas (Gingras et al., 1995; Vitolo et al., 1996), the relationship of integrin α6 expressing GBM cells with the vasculature remains unknown. To evaluate this relationship, we assessed GBM surgical biopsy specimens labeled with antibodies against integrin α6 and CD31, an endothelial cell marker. In concordance with the perivascular niche of GSCs (Calabrese et al, 2007), we detected high integrin α6 expression levels in these regions with infrequent co-expression with CD31 (Fig. 1A, A', B, B'), suggesting that these cells were not endothelial cells. 60% of integrin α6 positive GBM cells were located

within 5 μm of a blood vessel as compared to only 10% of total tumor cells (Supplementary Fig. 1A). Integrin α6 and CD133 were co-expressed in perivascular regions (Fig. 1C, C', D, D'). Similar perivascular co-expression patterns for integrin α6 and nestin were also evident (Supplementary Fig. 1B, B',C, C'). These findings were confirmed in freshly isolated GBM surgical biopsies, with a fraction of integrin α6 positive cells (1.1% and 15.9%, CCF1585, CCF1966) and dual flow cytometry analysis with CD133 indicated an overlap in expression which ranged from 0.1% - 11.3% of the total population (Fig. 1E). These data demonstrate that a fraction of GBM cells express integrin α6 located in the perivascular niche.

GSC express high levels of integrin α6

In GBM surgical biopsies, integrin α6 and CD133 expression levels were correlated. To evaluate GSC expression of integrin α6, GSCs were derived from human specimens amplified *in vivo* as previously described (Bao et al., 2008; Bao et al., 2006a; Bao et al., 2006b; Li et al., 2009). Functional assays to define GSCs included self-renewal assays, expression of stem cell markers, and tumor propagation. GSCs expressed significantly higher levels of integrin α6 mRNA compared to matched non-stem glioma cells by quantitative real time PCR (Fig. 2A). Reverse transcription PCR confirmed differential integrin α6 mRNA expression in GSCs with a similar pattern in expression of Olig2, another putative GSC marker (Fig. 2B). To evaluate the expression of integrin α6 and CD133 at the cellular level, we performed both flow cytometry and single cell immunoflourescence. We detected variations in the expression levels of integrin α6 and CD133, but the cellular populations expressing both antigens strongly overlapped (Fig. 1C, Supplementary Table 1). Integrin α6 was expressed in a greater percentage of GSCs as compared to non-stem glioma cells (Supplementary Fig. 2). To correlate the expression of integrin α6 with other GSC markers, we analyzed GSCs immediately after enrichment by immunofluorescence. Integrin α6, CD133, and Olig2 were co-expressed in the GSCs but in the non-GSC cell fraction (Fig. 2D). These results show that integrin α6 is enriched in the GSC population.

Integrin α6 expression co-segregates with GSC marker expression

To further assess the expression of integrin α6 with regard to other GSC markers, we cultured CD133-enriched GSCs as tumorspheres using previously reported proliferation conditions (Lee et al., 2006a). Cryosectioned spheres contained cellular populations that co-express integrin α6 and GSC markers Olig2 (Fig. 3A, D, G), CD133 (Fig. 3B, E, H), and nestin (Fig. 3C, F, I). Integrin α6 forms functional dimers with integrin β1 or β4, but we did not detect integrin β4 expression (data not shown) so we focused on integrin β1 expression. Integrin α6 expressing cells in tumorspheres expressed the integrin β1 co-receptor with proximal extracellular laminin ligand expression supporting the presence of a fully active integrin signaling unit (Fig. 4). Although leukemic stem cells display a quiescent phenotype, we and others have found that GSCs are proliferative. Indeed, integrin α6 positive cells in tumorspheres expressed the M-phase marker phospho-histone H3 (pH3) suggesting a cycling GSC (Supplementary Fig. 3A, B, C). Finally, we assessed the relationship between differentiation and cell survival of the integrin α6 population using the neuronal marker Map2 (Supplementary Fig. 3D, E, F) and the terminal deoxynucleotidyl transferase dUTP nick end labeling (TUNEL) assay (Supplementary Fig 3G), which detects DNA fragmentation as an indicator of apoptosis. We found that non-stem glioma cells and apoptotic cells do not express high levels of integrin α6. Collectively, these data show that integrin α6 co-segregates with GSC markers as well as the appropriate co-receptor and ligand.

Cell selection based on integrin α6 and CD133 expression enriches for cells with in vitro GSC properties

CD133 is not been absolutely informative in segregating tumor propagation requiring the development of additional CSC markers and suggesting that $CD133^{negative}$ cells with GSC properties may be identified with other markers. Based on this background, we assessed the utility of integrin α6 selection alone or in combination with CD133 to enrich for GSCs using fluorescence activated cell sorting (FACS). As demonstrated in Figure 1, double labeling of tumor specimens with integrin α6 and CD133 yields four populations. Cells from the $CD133^{positive}$;integrin $\alpha6^{hi}$ and $CD133^{negative}$;integrin $\alpha6^{hi}$ quadrants proliferated more than cells negative for integrin α6 (Fig. 5A, B). Tumorsphere formation assays, which are associated with self-renewal but are not an absolute indicator of self-renewal, showed that $CD133^{positive}$;integrin $\alpha6^{hi}$ and $CD133^{negative}$;integrin $\alpha6^{hi}$ formed spheres with significantly greater efficiency than cells negative for integrin α6 (Fig. 5C, D). These results demonstrate that integrin α6 expression is informative for cells with a higher propensity to proliferate and form tumorspheres in both $CD133^{positive}$ and $CD133^{negative}$ populations.

CD133 expression is not always detectable in all tumors and as such, we assessed the ability for integrin α6 to enrich for GSCs. We evaluated a tumor (D320MG) in which there is little CD133 expression (Supplementary Fig. 4A) and divided the expression level of integrin α6 into three compartments (low, medium, and high; Supplementary Fig. 4B). Cells that were integrin $\alpha6^{hi}$ (medium and high) displayed greater cell proliferation profile (Supplementary Fig. 4C) and increased tumorsphere formation than integrin $\alpha6^{lo}$ cells (Supplementary Fig. 4D). Cells with the highest level of integrin α6 expression (representing the top 50% of the integrin α6 expression) proliferated the most and formed secondary spheres with the greatest efficiency. These results demonstrate integrin α6 can be used to enrich for cells with in vitro GSC properties in a tumor which expresses little to no detectable levels of CD133.

Next we assessed the ability of integrin $\alpha6^{hi}$ and integrin $\alpha6^{lo}$ cells to undergo self-renewal in an *in vitro* setting. Tumor specimens were enriched or depleted based on integrin α6 expression levels and plated at single cell clonal density. Significantly more tumorspheres formed from the integrin $\alpha6^{hi}$ population (Fig. 5E, F). These results suggest that the majority of the cells which undergo self renewal are integrin $\alpha6^{hi}$ and confirm our data that demonstrated that integrin $\alpha6^{hi}$ cells (with or without high levels of CD133) are more likely to self-renew. We additionally queried if there were differences between the $CD133^{positive}$;integrin $\alpha6^{hi}$ and $CD133^{negative}$;integrin $\alpha6^{hi}$ cell populations. Tumorspheres were generated from each cell population and CD133 expression was assessed. $CD133^{positive}$ parental populations had greater CD133 expression than $CD133^{negative}$;integrin $\alpha6^{hi}$ parental populations (T08-0387: 13.5% integrin $\alpha6^{hi}$/ $CD133^{negative}$, 25.1% $CD133^{positive}$, 47% reduction; T3359: 11.3% integrin $\alpha6^{hi}$/ $CD133^{negative}$, 30.5% $CD133^{positive}$, 63% reduction; data not shown). These results demonstrate the utility of integrin α6 enrichment for GSCs, both in the presence and absence of CD133 expression. Another aspect of GSC biology is the ability to possess multi-lineage differentiation capacity. GBM cells were selected based on elevated integrin α6 expression level, expanded briefly, and then differentiated. Cells that originated from integrin $\alpha6^{hi}$ cells were capable of differentiating into all three CNS lineages: neurons, astrocytes, and oligodendrocytes (Supplementary Fig. 5). These studies confirm the ability of integrin $\alpha6^{hi}$ cells to both self-renew and differentiate into CNS lineages, demonstrating they possess stem-cell like properties.

Cell selection based on integrin α6 expression levels enriches for cells with in vivo GSC properties

The final property of GSCs, and arguably the most critical, is the ability to propagate secondary tumors. To evaluate if integrin α6 expression was indicative of a GSC phenotype, we enriched or depleted two separate tumors based on integrin α6 expression using FACS and performed in vivo limiting dilution transplantation assays. Cells enriched in integrin α6 expression (integrin $\alpha6^{hi}$), formed tumors at a significantly higher frequency and shorter time to tumor initiation than cells with integrin $\alpha6^{lo}$ expression (Figure 5G, H, Supplementary Table 2). In addition, fewer integrin $\alpha6^{hi}$ cells were required to initiate tumors that grew with a shorter latency compared to integrin $\alpha6^{lo}$ cells ($p = 0.0021$, Supplementary Table 2). These results, along with the tumorsphere formation and differentiation studies, demonstrate that cells which possess high levels of integrin α6 are capable of fulfilling the functional definition of a GSC.

Integrin α6 is critical to GSCs self-renewal and tumor formation

Given that integrin α6 is enriched in GSCs and that selection of bulk tumor cells based on integrin α6 expression yields cells with GSC properties, we hypothesized that integrin α6 functions to promote GSC maintenance. Lentivirus delivered short hairpin RNA (shRNA) constructs were designed against integrin α6 (shRNA 1 targeting exon 14 and shRNA 2 targeting exon 2). We validated integrin α6 knockdown in GSCs by FACS (Supplementary Fig. 6A). Targeting integrin α6 inhibited GSC cell growth (Fig. 6A, B) and abrogated tumorsphere formation (Fig 6C, Supplementary Fig. 6B, C). To determine the cellular mechanism, we assessed cell cycle progression and survival. GSCs transduced with shRNA against integrin α6 underwent cell cycle arrest and increased cell death. Cell cycle analysis showed an increase in the G_1 fraction and a decrease in S-phase fractions for cells targeted with integrin α6 shRNA (Supplementary Fig. 6D, E). The decrease in S-phase was confirmed using 5-ethynyl-2′-deoxyuridine (EdU) incorporation (Fig. 6D). Cell death increased upon integrin α6 targeting as assessed by caspase 3/7 activation (Fig. 6F, Supplementary Fig. 6F, G) and DNA fragmentation (Fig. 7E) assays. Interestingly, targeting integrin α6 in the $CD133^{negative}$;integrin $\alpha6^{hi}$ cell fraction produced a similar phenotype with decreased tumorsphere formation (Supplementary Fig. 6H), decreased cell growth (Supplementary Fig. 6I), an increased in G_1 and decrease in S-phase of the cell cycle (Supplementary Fig. 6J), and increased cell death (Supplementary Fig. 6K, L) suggesting that integrin α6 contributes to cell growth regardless of CD133 expression. These results demonstrate that targeting of integrin α6 in $CD133^{positive}$;integrin $\alpha6^{hi}$ and $CD133^{negative}$;integrin $\alpha6^{hi}$ cells results in a compromised GSC phenotype.

Next, we evaluated whether disruption of integrin α6 function decreases tumor formation. To achieve this, we infected GSCs (T3359 $CD133^{positive}$ cells cultured short term) with a lentivirus delivering shRNA directed against integrin α6 or a non-targeting control and then transplanted either 1000 or 5000 cells into the brains of immunocompromised mice. Mice bearing integrin α6 shRNA GSCs showed significantly reduced tumor formation (Fig. 6G) and greater median survival (Supplementary Table 3) as compared with non-targeting control GSCs (representative tumor shown in Fig. 6H). These results suggest that integrin α6 is a regulator of tumor growth and functional knockdown of this signaling pathway reduces tumor formation.

Integrin function has been disrupted with a number of blocking antibodies and peptides, some of which have entered into clinical trials. To interrogate a potentially translatable targeting of integrin α6, we utilized an integrin α6 blocking antibody to evaluate integrin α6 function in GSCs. GSCs treated with the blocking antibody displayed reduced cell proliferation (Fig. 7A, B) and tumorsphere formation (Fig. 7C) compared with an isotype

control antibody. In addition, we transplanted GSCs treated with the blocking antibody into the brains of immunocompriomised mice. Mice bearing cells incubated with an isotype control antibody showed consistent tumor formation while mice bearing cells incubated with the blocking antibody displayed greater tumor latency ($p = 0.0027$ for T4597 and $p = 0.0143$ for T4302; Fig. 7D, Supplementary Table 4). As a final confirmation of the clinical relevance of integrin α6, we interrogated an in silico GBM patient database and found that integrin α6 expression inversely correlates with survival ($p = 0.0129$, Supplementary Fig. 7). Taken together, our results show that integrin α6 expression is elevated in GSCs, can be used for GSC enrichment, and regulates aspects of their phenotype.

Discussion

In this study, we have identified an ECM receptor, integrin α6, as being highly expressed in the GSC population. We observed that selection based on integrin α6 expression alone, or in combination with CD133, results in an enrichment of the GSC population from bulk tumor. These data also demonstrate that other markers can be used along with CD133 to enrich for GSCs (previously reported for L1CAM (Bao et al., 2008), A2B5 (Ogden et al., 2008), and CD15 (Son et al., 2009)). In addition, we show that the level of integrin α6 expression alone can be used as a measure GSC potential, which has also been used for normal stem cells (Hall et al., 2006). Our findings demonstrate that integrin α6 can be used to enrich for GSCs as well are serve as a potential therapeutic target and underscores the need to further evaluation of CSC niches in order to identify additional markers and therapeutic cites.

The prospective isolation of GSCs from bulk tumors remains a critical, unresolved issue. GBMs display remarkable heterogeneity so it is unlikely that a single marker or even a collection of markers (an immunophenotype) will absolutely enrich for GSCs. However, our data suggests that integrin α6 does inform the GSC phenotype. In addition, integrin α6 contributes to tumor cell proliferation, survival, self renewal, and in vivo growth. The role of integrin α6 is complex as we detect heterogeneity in the expression of both CD133 and integrin α6 and GSCs may express both CD133 and integrin α6 or possibly integrin α6 alone as integrin α6 single positive cell populations can proliferate and self renew. This is not a unique challenge in solid tumor stem cell markers as the uniformity of information contained in CSC markers remains an unresolved question in the CSC field. For example, in breast cancer, the $CD44^{hi}CD24^{lo}$ immunophenotype enriches for CSCs as does $ALDH^{hi}$ yet these cellular pools only overlap to a minor degree in many tumors (Ginestier et al., 2007). Even within a single tumor, different pools of CSCs may be present (Piccirillo et al., 2009). It is therefore likely that tumors have variability not only in the fraction of $CD133^{positive}$ and integrin $\alpha6^{hi}$ cells but also in how these populations overlap and the potential that some variances in how they mark GSCs. The generalizability of our studies may be supported by a combination of data from GBM surgical biopsy specimens that have been previously demonstrated to be an accurate model of the human disease. We have amplified some tumors as xenografts, which we and others have shown to maintain their tumorgenic potential and relative marker expression (Bao et al., 2006a; Shu et al., 2008; Son et al., 2009). The correlation between integrin α6 and CD133 expression observed in xenografts by flow cytometry and immunostaining from T3359 and T3691 specimens was also observed in the original GBM biopsies (Supplementary Fig. 1D, D', E, E').

The perivascular localization of integrin α6 provides additional substantiation to the importance of the vasculature GSC maintenance. Our studies add an additional mechanism in the interplay between CSCs and the tumor vasculature. Previous studies have demonstrated that growth factors (Bao et al., 2006b) and cell-to-cell signaling (Calabrese et al., 2007) are regulators of GSCs, and we now demonstrate that the ECM present in the perivascular compartment maintains GSC via integrin α6. The ECM provides both structural

and instructive cues to normal neural stem cells (Lathia et al., 2007a) within the CNS. Several reports have suggested that ECM structures originating from blood vessels in the adult neural stem cell germinal zones are critical in preserving their maintenance through serving as a reservoir for growth factors (Kerever et al., 2007). The amplification of limited growth factor concentrations is an underappreciated function of the ECM and in GBMs, may play a vital role in trapping the secreted factors aiding in the preservation of GSC maintenance.

A potential clinical significance of our findings is derived from the ability of targeting integrin α6 in GSCs via blocking antibodies or lentivirus delivered shRNA to compromise self renewal and tumor initiation potential. *In vivo* studies demonstrated that integrin α6 blockade increased tumor latency and survival suggesting that integrin α6 is playing a role in tumor propagation, and in some instance tumor initiation. Dissecting the impact of integrin α6 on tumor initiation versus propagation is a critical question but it not possible with current *in vivo* assays. Our data are consistent with previous reports showing that CSC specific therapies may reduce tumor growth without an absolute termination of tumor growth (Hoey et al., 2009) and underscore the development of multimodal therapies that integrate both convention and CSC therapeutic approaches. Our results further suggest that RNA interference approaches for the integrins may require further development as we were unable to completely silence integrin α6 expression as shown by flow cytometry analysis (Supplementary Fig. 6A). In addition, the tumors that formed from integrin α6 lentivirus targeted GSCs showed expression of integrin α6 (Supplementary Fig 6M), suggesting the lentiviral knockdown of integrin α6 is not completely efficient or may be silenced. One limitation of integrin targeting alone may be the long half life of the protein (hours to days, depending on the context). RNA inference may be useful in combinatorial treatment paradigms with neutralizing antibodies or conventional cytotoxic therapies, such as radiation and temozolomide. Another possible therapeutic combination strategy would target the vasculature with anti-angiogenics (e.g. bevacizumab (Bao et al., 2006b) or vascular disruptive agents as integrin α6 has recently been reported to have a combined effect with VEGF in human brain microvascular cells (Lee et al., 2006b). To maximize a therapeutic index, the design of such therapies must take into consideration the integrin α6 expression throughout the brain, even if the integrin targeting is confined to a focal region. Integrin α6 is highly expressed by neural stem cells in rodents (Campos et al., 2004; Lathia et al., 2007a) and humans (Hall et al., 2006). In the adult murine brain, integrin α6 expression has been reported in the neural stem cell compartment adjacent to the lateral ventricles (Shen et al., 2008) and a detailed analysis suggests that the proliferating cells express integrin α6 as do the neural stem cell upon activation (I Kazanis, JD Lathia, C ffrench-Constant, unpublished observation). In addition, integrin α6 is expressed by embryonic and adult astrocytes, with levels being modulated in a cytokine dependent manner (Aloisi et al., 1992; Paulus et al., 1993).

While the exact pathway to which integrin α6 is driving the GSC phenotype is yet to be determined, it is likely to involve common downstream molecules of integrins such as Akt and c-myc, which we and others recently showed were also critical in GSC maintenance (Eyler et al., 2008; Wang et al., 2008b; Zheng et al., 2008). Aside from maintenance, disrupted integrin α6 could expose a survival requirement for GSC. It was recently shown in neural stem cells that addition of laminin to the culture media increased neurosphere formation and survival (Hall et al., 2008). Ablation of integrin α6 may compromise cell survival pathways in GSCs. Taken together, these data underscore the importance of integrin signaling within GBMs as targeting other integrins have shown promise (e.g. Cilengitide, an inhibitor of integrins αvβ3 and αvβ5, is currently in clinical trials (Reardon et al., 2008)) and suggest that GSC may preferentially have higher levels in integrins.

In summary, we show that GSCs have elevated levels of integrin α6, which can be used as an enrichment strategy alone or in combination with CD133. In addition, targeting integrin α6 has profound consequences on the GSC phenotype and may provide a therapeutic target for GBMs.

Experimental Procedures

GSC Isolation

GSCs were isolated from primary surgical GBM biopsy specimens in accordance with protocols approved by the Duke University Medical Center or Cleveland Clinic Foundation Institutional Review Boards. GSCs were used immediately after dissociation or after transient xenograft passage in immunocompromised mice. Cells were sorted into marker + and - populations using a CD133/2-APC conjugated antibody (293C3, Miltenyi Biotech) or an integrin α6-FITC antibody (55735, BD Biosciences) by fluorescence-activated cell sorting (FACS) or magnetic bead separation based on CD133 as previously described (Eyler et al., 2008; Wang et al., 2008b).

PCR analyses

Real time PCR analysis was done as previously described (Wang et al., 2008b). Real-time PCR was performed on an ABI 7900HT system using SYBR-Green Mastermix (SA Biosciences). The threshold cycle (C_T) values for each gene were normalized to expression levels of β-Actin. The primers used were as follows:

Integrin α6	ATTCTCATGCGAGCCTTCAT GGAAACACAGTCACTCGAACC
β-actin	AGAAAATCTGGCACCACACC AGAGGCGTACAGGGATAGCA

Reverse transcription PCR was following manufacturer's protocols. The sequences of the PCR primers are as follows:

Integrin α6	CTCGGCACAGCAACCTTGAACATT TGAGCATGGATCTCAGCCTTGTGA
Olig2	ATCTGGGTCAATCCACACCCTCTT ACAGCTTAGCATTGCGCACTTACC

Immunofluorescence

For immunostaining analyses, surgical GBM biopsy specimens were fixed for with 4% PFA for 10 minutes at room temperature. Cells or sections were blocked with a PBS based solution containing 10% normal goat serum (Sigma) and 0.1% triton x-100 (Sigma). Sections or cells were incubated overnight with the appropriate primary antibody at 4°C and then washed with PBS three times prior to incubation with the appropriate secondary antibody for 45 minutes at room temperature. Prior to coverslip application, nuclei were counterstained with Hoechst and imaging done using a Leica SP-5 confocal microscope as described previously (Wang et al., 2008b).

In vivo tumor initiation analysis

In vivo tumor initiation analyses were done with BALB/c nu/nu mice under a Cleveland Clinic Foundation Institutional Animal Care and Use Committee–approved protocol as previously described (Bao et al., 2006b, Wang et al., 2008b). All transplanted mice were maintained for 100 days or until development of neurologic signs.

Statistical Analysis

Values are reported as the mean +/− the standard error. GraphPad Instat 3 Software (GraphPad Software, Inc.) was used to determine statistical significance with either two-tailed Student's t-test or ANOVA as indicated. Significance testing of survival was performed by log-rank analysis.

Supplementary Material

Refer to Web version on PubMed Central for supplementary material.

Acknowledgments

We thank Dr. Mike Cook, Dr. Beth Harvat, Cathy Shemo, Moneen Morgan, and Sage O'Bryant for flow cytometry assistance, Linda Vargo for histology assistance, and the members of the Rich laboratory for technical assistance and critical review of the manuscript. We are also grateful to Dr. Michael Forrester for advice on the DNA fragmentation assay. We are also grateful to Drs. Mahendra S. Rao, Richard Ransohoff, Thomas Egelhoff, Yogen Saunthararajah, and Jeongwu Lee for valuable insight and comments on the manuscript. Work in the Rich laboratory is supported by the Childhood Brain Tumor Foundation, the Pediatric Brain Tumor Foundation of the United States, Accelerate Brain Cancer Cure, Alexander and Margaret Stewart Trust, Brain Tumor Society, Goldhirsh Foundation, Duke Comprehensive Cancer Center Stem Cell Initiative Grant, and NIH grants NS047409, NS054276, CA112958, and CA116659. J.N.R. is a Damon Runyon-Lilly Clinical Investigator supported by the Damon Runyon Cancer Research Foundation and a Sidney Kimmel Foundation for Cancer Research Scholar. A.H. is supported by the National Brain Tumor Society. C.E.E. is supported by a National Research Service Award from the National Institutes of Neurological Disorders and Stroke (NINDS F30 NS063496). J.D.L. is supported by an American Brain Tumor Association Basic Research Fellowship (sponsored by the Joelle Syverson Fund) and a National Service Research Award (NCI F32 CA142159). The Duke University Brain Tumor Tissue Bank is supported by the Duke University Brain Cancer SPORE, and we thank D. Satterfield, L. Ehinger, J. Funkhouser, and J. Faison for technical assistance. Studies were also supported by the Cleveland Clinic Foundation Tissue Procurement Service, and we thank S. Staugatis, R. Weil, and M. McGraw for their assistance.

References

Aloisi F, Borsellino G, Samoggia P, Testa U, Chelucci C, Russo G, Peschle C, Levi G. Astrocyte cultures from human embryonic brain: characterization and modulation of surface molecules by inflammatory cytokines. Journal of neuroscience research 1992;32:494–506. [PubMed: 1356158]

Bao S, Wu Q, Li Z, Sathornsumetee S, Wang H, McLendon RE, Hjelmeland AB, Rich JN. Targeting cancer stem cells through L1CAM suppresses glioma growth. Cancer Res 2008;68:6043–6048. [PubMed: 18676824]

Bao S, Wu Q, McLendon RE, Hao Y, Shi Q, Hjelmeland AB, Dewhirst MW, Bigner DD, Rich JN. Glioma stem cells promote radioresistance by preferential activation of the DNA damage response. Nature 2006a;444

Bao S, Wu Q, Sathornsumetee S, Hao Y, Li Z, Hjelmeland AB, Shi Q, McLendon RE, Bigner DD, Rich JN. Stem cell-like glioma cells promote tumor angiogenesis through vascular endothelial growth factor. Cancer Res 2006b;66:7843–7848. [PubMed: 16912155]

Bar EE, Chaudhry A, Lin A, Fan X, Schreck K, Matsui W, Piccirillo S, Vescovi AL, DiMeco F, Olivi A, Eberhart CG. Cyclopamine-mediated hedgehog pathway inhibition depletes stem-like cancer cells in glioblastoma. Stem cells (Dayton, Ohio) 2007;25:2524–2533.

Beier D, Hau P, Proescholdt M, Lohmeier A, Wischhusen J, Oefner PJ, Aigner L, Brawanski A, Bogdahn U, Beier CP. CD133(+) and CD133(−) glioblastoma-derived cancer stem cells show

differential growth characteristics and molecular profiles. Cancer Res 2007;67:4010–4015. [PubMed: 17483311]

Bidlingmaier S, Zhu X, Liu B. The utility and limitations of glycosylated human CD133 epitopes in defining cancer stem cells. Journal of molecular medicine (Berlin, Germany) 2008;86:1025–1032.

Calabrese C, Poppleton H, Kocak M, Hogg TL, Fuller C, Hamner B, Oh EY, Gaber MW, Finklestein D, Allen M, et al. A perivascular niche for brain tumor stem cells. Cancer cell 2007;11:69–82. [PubMed: 17222791]

Campos LS, Leone DP, Relvas JB, Brakebusch C, Fassler R, Suter U, ffrench-Constant C. Beta1 integrins activate a MAPK signalling pathway in neural stem cells that contributes to their maintenance. Development 2004;131:3433–3444. [PubMed: 15226259]

Eyler CE, Foo WC, Lafiura KM, McLendon RE, Hjelmeland AB, Rich JN. Brain Cancer Stem Cells Display Preferential Sensitivity to Akt Inhibition. Stem cells (Dayton, Ohio). 2008

Fael Al-Mayhani TM, Ball SL, Zhao JW, Fawcett J, Ichimura K, Collins PV, Watts C. An efficient method for derivation and propagation of glioblastoma cell lines that conserves the molecular profile of their original tumours. J Neurosci Methods 2009;176:192–199. [PubMed: 19215724]

Fan X, Matsui W, Khaki L, Stearns D, Chun J, Li YM, Eberhart CG. Notch pathway inhibition depletes stem-like cells and blocks engraftment in embryonal brain tumors. Cancer Res 2006;66:7445–7452. [PubMed: 16885340]

Fortunel NO, Otu HH, Ng HH, Chen J, Mu X, Chevassut T, Li X, Joseph M, Bailey C, Hatzfeld JA, et al. Comment on " 'Stemness': transcriptional profiling of embryonic and adult stem cells" and "a stem cell molecular signature". Science 2003;302:393. author reply 393. [PubMed: 14563990]

Galli R, Binda E, Orfanelli U, Cipelletti B, Gritti A, De Vitis S, Fiocco R, Foroni C, Dimeco F, Vescovi A. Isolation and characterization of tumorigenic, stem-like neural precursors from human glioblastoma. Cancer Res 2004;64:7011–7021. [PubMed: 15466194]

Georges-Labouesse E, Mark M, Messaddeq N, Gansmuller A. Essential role of alpha 6 integrins in cortical and retinal lamination. Curr Biol 1998;8:983–986. [PubMed: 9742403]

Gilbertson RJ, Rich JN. Making a tumour's bed: glioblastoma stem cells and the vascular niche. Nature reviews 2007;7:733–736.

Ginestier C, Hur MH, Charafe-Jauffret E, Monville F, Dutcher J, Brown M, Jacquemier J, Viens P, Kleer CG, Liu S, et al. ALDH1 is a marker of normal and malignant human mammary stem cells and a predictor of poor clinical outcome. Cell stem cell 2007;1:555–567. [PubMed: 18371393]

Gingras MC, Roussel E, Bruner JM, Branch CD, Moser RP. Comparison of cell adhesion molecule expression between glioblastoma multiforme and autologous normal brain tissue. J Neuroimmunol 1995;57:143–153. [PubMed: 7535788]

Graus-Porta D, Blaess S, Senften M, Littlewood-Evans A, Damsky C, Huang Z, Orban P, Klein R, Schittny JC, Muller U. Beta1-class integrins regulate the development of laminae and folia in the cerebral and cerebellar cortex. Neuron 2001;31:367–379. [PubMed: 11516395]

Hall PE, Lathia JD, Caldwell MA, Ffrench-Constant C. Laminin enhances the growth of human neural stem cells in defined culture media. BMC Neurosci 2008;9:71. [PubMed: 18651950]

Hall PE, Lathia JD, Miller NG, Caldwell MA, ffrench-Constant C. Integrins are markers of human neural stem cells. Stem cells (Dayton, Ohio) 2006;24:2078–2084.

Hanahan D, Weinberg RA. The hallmarks of cancer. Cell 2000;100:57–70. [PubMed: 10647931]

Hemmati HD, Nakano I, Lazareff JA, Masterman-Smith M, Geschwind DH, Bronner-Fraser M, Kornblum HI. Cancerous stem cells can arise from pediatric brain tumors. Proc Natl Acad Sci U S A 2003;100:15178–15183. [PubMed: 14645703]

Hoey T, Yen WC, Axelrod F, Basi J, Donigian L, Dylla S, Fitch-Bruhns M, Lazetic S, Park IK, Sato A, et al. DLL4 blockade inhibits tumor growth and reduces tumor-initiating cell frequency. Cell stem cell 2009;5:168–177. [PubMed: 19664991]

Hynes RO. Integrins: bidirectional, allosteric signaling machines. Cell 2002;110:673–687. [PubMed: 12297042]

Ignatova TN, Kukekov VG, Laywell ED, Suslov ON, Vrionis FD, Steindler DA. Human cortical glial tumors contain neural stem-like cells expressing astroglial and neuronal markers in vitro. Glia 2002;39:193–206. [PubMed: 12203386]

Jaksch M, Munera J, Bajpai R, Terskikh A, Oshima RG. Cell cycle-dependent variation of a CD133 epitope in human embryonic stem cell, colon cancer, and melanoma cell lines. Cancer Res 2008;68:7882–7886. [PubMed: 18829544]

Joo KM, Kim SY, Jin X, Song SY, Kong DS, Lee JI, Jeon JW, Kim MH, Kang BG, Jung Y, et al. Clinical and biological implications of CD133-positive and CD133-negative cells in glioblastomas. Lab Invest 2008;88:808–815. [PubMed: 18560366]

Kerever A, Schnack J, Vellinga D, Ichikawa N, Moon C, Arikawa-Hirasawa E, Efird JT, Mercier F. Novel extracellular matrix structures in the neural stem cell niche capture the neurogenic factor fibroblast growth factor 2 from the extracellular milieu. Stem cells (Dayton, Ohio) 2007;25:2146–2157.

Lathia JD, Patton B, Eckley DM, Magnus T, Mughal MR, Sasaki T, Caldwell MA, Rao MS, Mattson MP, ffrench-Constant C. Patterns of laminins and integrins in the embryonic ventricular zone of the CNS. J Comp Neurol 2007a;505:630–643. [PubMed: 17948866]

Lathia JD, Rao MS, Mattson MP, Ffrench-Constant C. The microenvironment of the embryonic neural stem cell: lessons from adult niches? Dev Dyn 2007b;236:3267–3282. [PubMed: 17937403]

Lee J, Kotliarova S, Kotliarov Y, Li A, Su Q, Donin NM, Pastorino S, Purow BW, Christopher N, Zhang W, et al. Tumor stem cells derived from glioblastomas cultured in bFGF and EGF more closely mirror the phenotype and genotype of primary tumors than do serum-cultured cell lines. Cancer cell 2006a;9:391–403. [PubMed: 16697959]

Lee TH, Seng S, Li H, Kennel SJ, Avraham HK, Avraham S. Integrin regulation by vascular endothelial growth factor in human brain microvascular endothelial cells: role of alpha6beta1 integrin in angiogenesis. J Biol Chem 2006b;281:40450–40460. [PubMed: 17085437]

Li Z, Bao S, Wu Q, Wang H, Eyler C, Sathornsumetee S, Shi Q, Cao Y, Lathia J, McLendon RE, et al. Hypoxia-inducible factors regulate tumorigenic capacity of glioma stem cells. Cancer cell 2009;15:501–513. [PubMed: 19477429]

Liu G, Yuan X, Zeng Z, Tunici P, Ng H, Abdulkadir IR, Lu L, Irvin D, Black KL, Yu JS. Analysis of gene expression and chemoresistance of CD133+ cancer stem cells in glioblastoma. Mol Cancer 2006;5

Loulier K, Lathia JD, Marthiens V, Relucio J, Mughal MR, Tang SC, Coksaygan T, Hall PE, Chigurupati S, Patton B, et al. beta1 integrin maintains integrity of the embryonic neocortical stem cell niche. PLoS Biol 2009;7:e1000176. [PubMed: 19688041]

Ogden AT, Waziri AE, Lochhead RA, Fusco D, Lopez K, Ellis JA, Kang J, Assanah M, McKhann GM, Sisti MB, et al. Identification of A2B5+CD133-tumor-initiating cells in adult human gliomas. Neurosurgery 2008;62:505–514. discussion 514-505. [PubMed: 18382330]

Patrawala L, Calhoun-Davis T, Schneider-Broussard R, Tang DG. Hierarchical organization of prostate cancer cells in xenograft tumors: the CD44+alpha2beta1+ cell population is enriched in tumor-initiating cells. Cancer Res 2007;67:6796–6805. [PubMed: 17638891]

Paulus W, Baur I, Schuppan D, Roggendorf W. Characterization of integrin receptors in normal and neoplastic human brain. The American journal of pathology 1993;143:154–163. [PubMed: 8317546]

Piccirillo SG, Combi R, Cajola L, Patrizi A, Redaelli S, Bentivegna A, Baronchelli S, Maira G, Pollo B, Mangiola A, et al. Distinct pools of cancer stem-like cells coexist within human glioblastomas and display different tumorigenicity and independent genomic evolution. Oncogene 2009;28:1807–1811. [PubMed: 19287454]

Piccirillo SG, Reynolds BA, Zanetti N, Lamorte G, Binda E, Broggi G, Brem H, Olivi A, Dimeco F, Vescovi AL. Bone morphogenetic proteins inhibit the tumorigenic potential of human brain tumour-initiating cells. Nature 2006;444:761–765. [PubMed: 17151667]

Pollard SM, Yoshikawa K, Clarke ID, Danovi D, Stricker S, Russell R, Bayani J, Head R, Lee M, Bernstein M, et al. Glioma stem cell lines expanded in adherent culture have tumor-specific phenotypes and are suitable for chemical and genetic screens. Cell stem cell 2009;4:568–580. [PubMed: 19497285]

Read TA, Fogarty MP, Markant SL, McLendon RE, Wei Z, Ellison DW, Febbo PG, Wechsler-Reya RJ. Identification of CD15 as a marker for tumor-propagating cells in a mouse model of medulloblastoma. Cancer cell 2009;15:135–147. [PubMed: 19185848]

Reardon DA, Fink KL, Mikkelsen T, Cloughesy TF, O'Neill A, Plotkin S, Glantz M, Ravin P, Raizer JJ, Rich KM, et al. Randomized phase II study of cilengitide, an integrin-targeting arginine-glycine-aspartic acid peptide, in recurrent glioblastoma multiforme. J Clin Oncol 2008;26:5610–5617. [PubMed: 18981465]

Reya T, Morrison SJ, Clarke MF, Weissman IL. Stem cells, cancer, and cancer stem cells. Nature 2001;414:105–111. [PubMed: 11689955]

Schmid RS, Anton ES. Role of integrins in the development of the cerebral cortex. Cereb Cortex 2003;13:219–224. [PubMed: 12571112]

Shen Q, Wang Y, Kokovay E, Lin G, Chuang SM, Goderie SK, Roysam B, Temple S. Adult SVZ stem cells lie in a vascular niche: a quantitative analysis of niche cell-cell interactions. Cell stem cell 2008;3:289–300. [PubMed: 18786416]

Shu Q, Wong KK, Su JM, Adesina AM, Yu LT, Tsang YT, Antalffy BC, Baxter P, Perlaky L, Yang J, et al. Direct orthotopic transplantation of fresh surgical specimen preserves CD133+ tumor cells in clinically relevant mouse models of medulloblastoma and glioma. Stem cells (Dayton, Ohio) 2008;26:1414–1424.

Singh SK, Clarke ID, Terasaki M, Bonn VE, Hawkins C, Squire J, Dirks PB. Identification of a cancer stem cell in human brain tumors. Cancer Res 2003;63:5821–5828. [PubMed: 14522905]

Singh SK, Hawkins C, Clarke ID, Squire JA, Bayani J, Hide T, Henkelman RM, Cusimano MD, Dirks PB. Identification of human brain tumour initiating cells. Nature 2004;432:396–401. [PubMed: 15549107]

Son MJ, Woolard K, Nam DH, Lee J, Fine HA. SSEA-1 is an enrichment marker for tumor-initiating cells in human glioblastoma. Cell stem cell 2009;4:440–452. [PubMed: 19427293]

Taylor MD, Poppleton H, Fuller C, Su X, Liu Y, Jensen P, Magdaleno S, Dalton J, Calabrese C, Board J, et al. Radial glia cells are candidate stem cells of ependymoma. Cancer cell 2005;8:323–335. [PubMed: 16226707]

Uchida N, Buck DW, He D, Reitsma MJ, Masek M, Phan TV, Tsukamoto AS, Gage FH, Weissman IL. Direct isolation of human central nervous system stem cells. Proc Natl Acad Sci U S A 2000;97:14720–14725. [PubMed: 11121071]

Vaillant F, Asselin-Labat ML, Shackleton M, Forrest NC, Lindeman GJ, Visvader JE. The mammary progenitor marker CD61/beta3 integrin identifies cancer stem cells in mouse models of mammary tumorigenesis. Cancer Res 2008;68:7711–7717. [PubMed: 18829523]

Vitolo D, Paradiso P, Uccini S, Ruco LP, Baroni CD. Expression of adhesion molecules and extracellular matrix proteins in glioblastomas: relation to angiogenesis and spread. Histopathology 1996;28:521–528. [PubMed: 8803595]

Wang J, Sakariassen PO, Tsinkalovsky O, Immervoll H, Boe SO, Svendsen A, Prestegarden L, Rosland G, Thorsen F, Stuhr L, et al. CD133 negative glioma cells form tumors in nude rats and give rise to CD133 positive cells. International journal of cancer 2008a;122:761–768.

Wang J, Wang H, Li Z, Wu Q, Lathia JD, McLendon RE, Hjelmeland AB, Rich JN. c-Myc is required for maintenance of glioma cancer stem cells. PloS one 2008b;3:e3769. [PubMed: 19020659]

Yuan X, Curtin J, Xiong Y, Liu G, Waschsmann-Hogiu S, Farkas DL, Black KL, Yu JS. Isolation of cancer stem cells from adult glioblastoma multiforme. Oncogene 2004;23:9392–9400. [PubMed: 15558011]

Zheng H, Ying H, Yan H, Kimmelman AC, Hiller DJ, Chen AJ, Perry SR, Tonon G, Chu GC, Ding Z, et al. p53 and Pten control neural and glioma stem/progenitor cell renewal and differentiation. Nature 2008;455:1129–1133. [PubMed: 18948956]

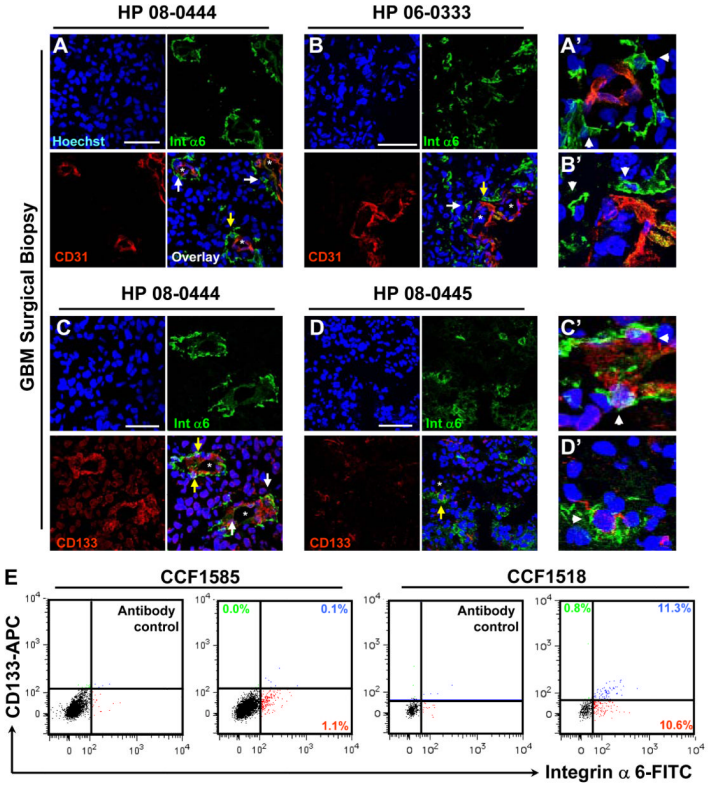

Figure 1. Integrin α6 is expressed in human GBM cells and localized to the perivascular compartment

Immunostaining of GBM surgical biopsies (HP 08-0444, HP 06-033, HP 08-0445) demonstrates that integrin α6 (green) is expressed in the perivascular compartment (double stained with CD31 in red, **A, B**) and is co-expressed with CD133 (red, **C, D**). Blood vessels marked with an "*", regions of interest marked with a white arrow, and enlarged regions of interest marked with yellow arrow and shown in **A'-D'**. All nuclei counterstained with Hoechst in blue. Scale bar represents 50 μm. Flow cytometry analysis (**E**) indicates that integrin α6 is expressed in a fraction of cells in primary surgical GBM biopsies 18 hours after isolation (CCF1585) or after short term culture (CCF1518) with varying overlap with CD133 expression.

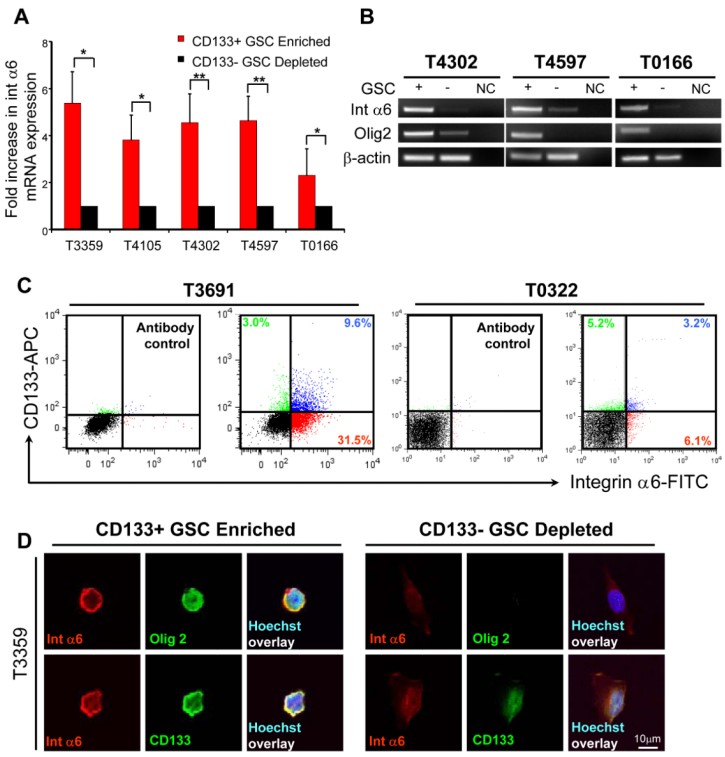

Figure 2. Integrin α6 is co-expressed with CD133-positive GSCs

(**A**) Quantitative PCR from tumor xenografts (T3359, T4105, T4302, T4597, T0166) indicates that in CD133 enriched GSC enriched populations, integrin α6 is also highly expressed in comparison to CD133 depleted non-stem glioma cells (n = 3, +/− S.E.M; *, $p < 0.05$; **, $p < 0.001$). (**B**) Reverse transcription PCR analysis demonstrates that integrin α6 and the GSC marker Olig2 are highly expressed in GSCs isolated from T4302, T4597, and T0166 tumor xenografts. NC, negative control (no cDNA added). (**C**) Flow cytometry analysis indicates that integrin α6 expression overlaps with CD133 expression in tumor xenografts (T3691, T0322). (**D**) Immunostaining analysis from tumor xenograft cells (T3359) immediately after CD133 enrichment show co-expression of CD133 positive cells with integrin α6 (red) and GSC markers CD133 (green) and Olig2 (green, nuclei counterstained in blue with Hoechst). CD133 negative cells show limited GSC or integrin α6 marker expression. Scale bar, 10 μm.

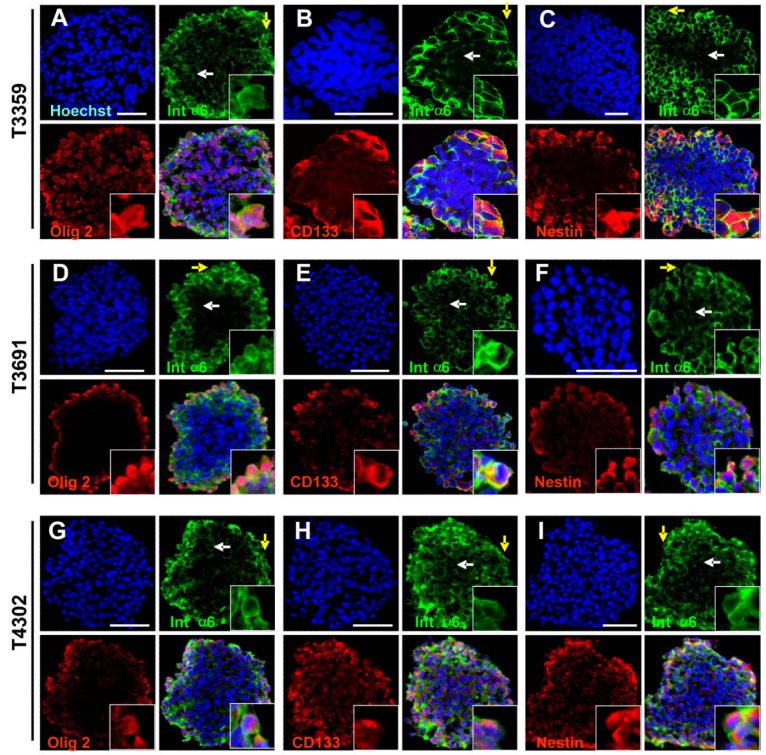

Figure 3. Integrin α6 co-segregates with CD133-positive GSCs

Immunostaining analysis of cryosections from tumorspheres generated from GSC enriched populations (T3359, T3691, T4302) show the peripheral region (yellow arrow, enlarged inset in bottom right corner) which appears to correlate with high integrin α6 expression and the inner region (white arrow), which is low in integrin α6 expression. Photomicrographs show integrin α6 (green) is co-expressed with GSC markers Olig2 (red, **A, D, E**), CD133 (red, **B, E, H**), and nestin (red, **C, F, I**). All nuclei counterstained with Hoechst in blue. Scale bar, 10 μm.

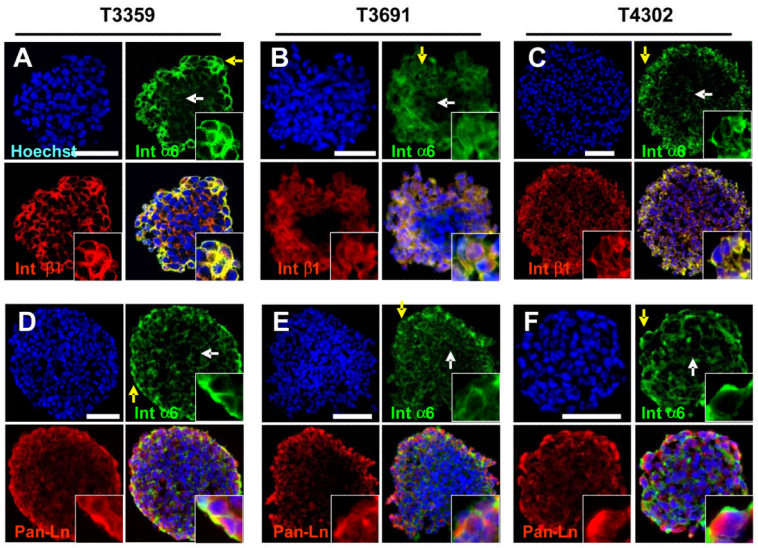

Figure 4. Integrin α6 segregates with co-receptor integrin β1 and ligand, laminin

Photomicrographs from tumorspheres generated from GSC enriched populations (T3359, T3691, T4302) show integrin α6 (green) is expressed with co-receptor integrin β1 (red, **A, B, C**) and ligand laminin (red, **C, D, E**) in the peripheral region (yellow arrow), but not the inner region (white arrow). All nuclei counterstained with Hoechst in blue. Scale bar, 50 μm.

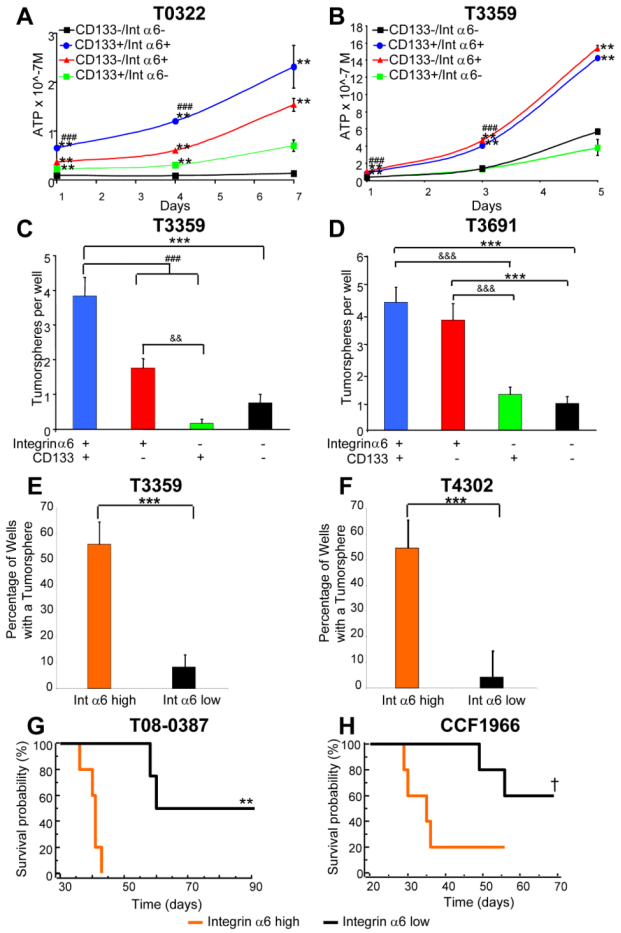

Figure 5. Selection of cells based on integrin α6 expression enriches for a population which display GSC properties

After GSC enrichment based on integrin α6 and CD133 expression, each cell population (black: $CD133^{negative}$/integrin $\alpha6^{lo}$, green: $CD133^{positive}$/integrin $\alpha6^{lo}$, red: $CD133^{negative}$/integrin $\alpha6^{hi}$, blue: $CD133^{positive}$/integrin $\alpha6^{hi}$) had a different growth profile. Cell titer assays demonstrated increased growth in integrin $\alpha6^{hi}$ cells isolated from T0322 (**A**) or T3359 (**B**) cells. **, $p < 0.01$ with ANOVA comparison to $CD133^{negative}$/integrin $\alpha6^{lo}$ cells at the same timepoint; ###, $p<0.001$ with ANOVA comparison of $CD133^{positive}$/integrin $\alpha6^{hi}$ cells to either $CD133^{positive}$/integrin $\alpha6^{lo}$ or $CD133^{negative}$/integrin $\alpha6^{hi}$ cells at the same timepoint. In tumorsphere formation assays for T3359 (**C**) and T3691 (**D**) cells, selection for CD133 and integrin α6 increased the number of tumorspheres per well. ***, $p < 0.001$ with ANOVA comparison to $CD133^{negative}$/integrin $\alpha6^{lo}$ cells; ###, $p<0.001$ with ANOVA comparison of $CD133^{positive}$/integrin $\alpha6^{hi}$ cells to either $CD133^{positive}$/integrin $\alpha6^{lo}$ or $CD133^{negative}$/integrin $\alpha6^{hi}$ cells; && $p < 0.01$ and &&&, $p<0.001$ with ANOVA comparison to $CD133^{positive}$/integrin $\alpha6^{lo}$ cells. GBM cells (from tumor specimens T3359, T4302) were sorted at a single cell per well based on integrin α6 expression. Graphs (**E, F**) indicate that cells selected from the integrin $\alpha6^{hi}$ high population (orange bar) formed tumorspheres at a significantly higher frequency than cells from the integrin $\alpha6^{lo}$ population (black bar, ***, $p < 0.001$). (**G, H**) Kaplan-Meier survival curves demonstrate decreased survival when cells high in integrin α6 expression are transplanted into the right frontal lobe of immunocompromised mice (†, $p < 0.067$ for 1000 CCF1966 cells; **, $p < 0.01$ for 500 T08-0387 cells ($p = 0.0051$) with log-rank analysis of survival curves).

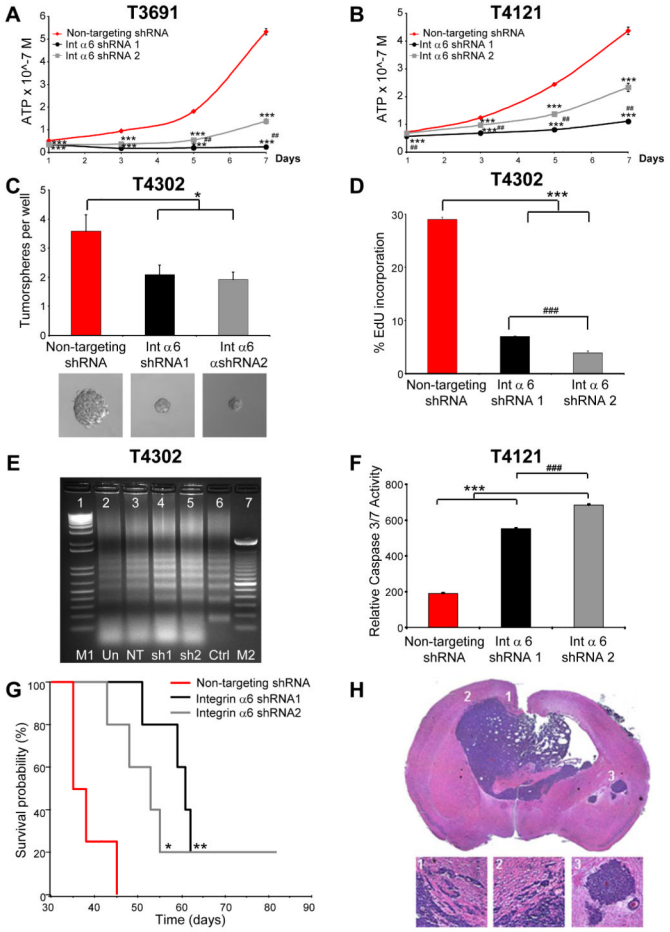

Figure 6. Integrin α6 knockdown results in a reduction in the GSC phenotype

Knockdown of integrin α6 using two separate lentiviral shRNA constructs results in a decreased cell proliferation profile as assessed by the cell titer assay in T3691 (**A**) and T4121 (**B**) xenograft tumor cells. ***, p<0.001 with ANOVA comparison to non-targeting shRNA at the same timepoint; ##, p<0,01 with ANOVA comparison of shRNA1 to shRNA2 at the same timepoint. (**C**) Quantification of the number of tumorspheres per well and representative pictures of tumorspheres demonstrates potential self-renewal was also impaired in GSC targeted with the lentivial shRNA constructs in T4302 cells. *, p < 0.05 with ANOVA comparison to non-targeting control. (**D**) EdU incorporation demonstrates a decrease in proliferative capacity T4302 cells using both shRNA constructs (*** p < 0.001 with ANOVA comparison to non-targeting control, ###, < 0.001 with ANOVA comparison to shRNA1). Knockdown of integrin α6 also increases cell death as assessed by a DNA fragmentation assay (**E**) on T4302 xenograft tumor cells (M1 = 1 kb ladder, Un = uninfected control, NT = non-targeting shRNA control, sh1=shRNA1, sh2=shRNA2, Ctrl = staurosporine control, M2 = 100 bp ladder). Cell death was also confirmed using a caspase 3/7 assay (**F**) on T4121 xenograft tumor cells (***, p < 0.001 with ANOVA comparison to non-targeting control; ###, p < 0.001 with ANOVA comparison to shRNA1). (**G**) Kaplan-Meier survival curve demonstrate increased survival when integrin α6 is targeted with shRNA in comparison to a non-targeting control. 1000 GSCs infected with integrin α6 shRNA targeting constructs or non-targeting control were intracranially transplanted into the right frontal lobe of immunocompromised mice. *, p < 0.05; **, p < 0.01 by log-rank analysis of survival curves. (**H**) Representative light micrograph showing H&E staining for

a control non-targeting integrin α6 1000 cell tumor showing characteristic bilateral tumor location, migrating edges, and secondary tumors, insets displayed below.

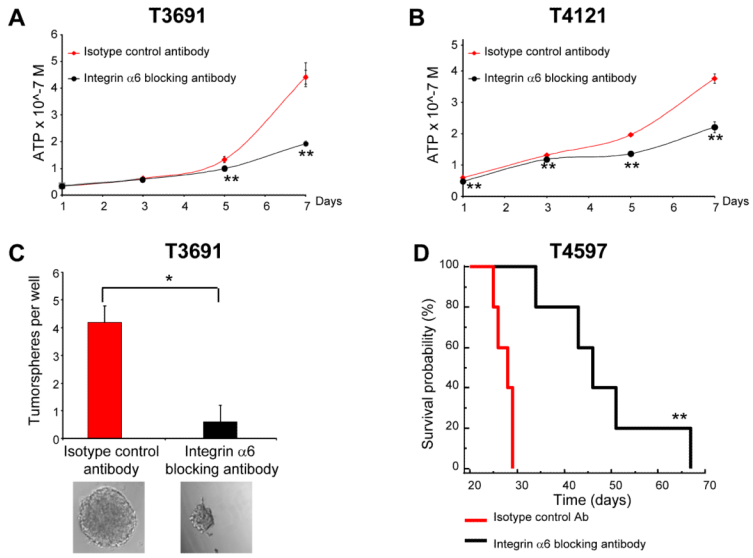

Figure 7. Integrin α6 blocking antibody results in a reduction in the GSC phenotype

This decrease in GSC proliferation was also seen using a blocking antibody to integrin α6 in T3691 (**A**) and T4121 (**B**) xenograft tumor cells in a concentration dependent manner as compared to an isotype control antibody. **, $p < 0.01$ with ANOVA comparison to isotype control at the same timepoint. (**C**) Tumorsphere formation is also inhibited by addition of the blocking antibody in T3359 xenograft tumor cells as shown by quantification of the number of tumorspheres per well and in representative images. *, $p < 0.01$. (**D**) Kaplan-Meier survival curve demonstrating increased survival when GSCs are incubated with the blocking antibody. 1000 integrin α6 + /CD133 - GSCs incubated with either a control or integrin α6 blocking antibody for five days and intracranially transplanted into the right frontal lobe of immunocompromised mice. **, $p < 0.01$ with log-rank analysis of survival curves.